Vietnam Journal of Science and Technology ***62*** *(2) (2024) 288-298*

doi:10.15625/2525-2518/18628

Aqueous synthesis of highly luminescent $AgInSe_2$/ZnS core/shell nanocrystals

Tran Thi Thu Huong[1], Nguyen Thi Hiep[2, 3], Nguyen Thu Loan[1], Le Van Long[1], Nguyen Thanh Tung[1], Ung Thi Dieu Thuy[1, *], Peter Reiss[4], Jae Yup Kim[5], Nguyen Quang Liem[1]

[1]*Institute of Materials Science, Vietnam Academy of Science and Technology, 18 Hoang Quoc Viet, Cau Giay, Ha Noi, Viet Nam*

[2]*Institute of Research and Development, Duy Tan University, Da Nang City, Viet Nam*

[3]*Faculty of Natural Sciences, Duy Tan University, Da Nang City, Viet Nam*

[4]*University of Grenoble Alpes, CEA, CNRS, IRIG-SyMMES, STEP, 38000 Grenoble, France*
[5]*Department of Chemical Engineering, Dankook University, Yongin, 16890, Republic of Korea*

[*]Email: *dieuthuy@ims.vast.vn*

Received: 7 August 2023; Accepted for publication: 27 February 2024

Abstract. Ternary I-III-VI chalcopyrite-type nanocrystals (NCs) range among the most important alternative materials to Cd-based NCs. Within this materials family, $AgInSe_2$ (AISe) presents a narrower bandgap than widely studied $AgInS_2$ (AIS), making it more suitable for numerous applications. At present, it remains a long-standing challenge to directly synthesize high-quality AISe core and AISe/ZnS core/shell NCs in aqueous solution at atmospheric pressure. In this work, we describe their synthesis using glutathione and citric acid as dual stabilizers. First, to form AISe core NCs, the Se precursor is injected into a solution containing the Ag and In complexes at 96 °C for 20 min. In the second step, the AISe/ZnS core/shell structure is created by growing the ZnS shell on the AISe NCs surface at 90 °C for 60 min. The synthesized AISe and AISe/ZnS core/shell NCs are characterized using X-ray diffraction, transmission electron microscopy, and UV-Vis absorption and photoluminescence for optical spectroscopies. After the growth of the ZnS shell, AISe/ZnS core/shell NCs exhibit higher photostability and emit intense luminescence at a wavelength of 680 nm with an impressive quantum yield (QY) of 30 %, which represents a threefold higher than the AISe core NCs. These properties make the aqueous soluble AISe/ZnS core/shell NCs favorable candidates for lighting, displays, and biological imaging applications.

Keywords: $AgInSe_2$, $AgInSe_2$/ZnS core/shell nanocrystals, water-soluble, photoluminescence, air-stable

Classification numbers: 2.1.1, 2.4.1, 2.10

1. INTRODUCTION

Ternary I–III–VI semiconductor nanocrystals (e.g. $CuInS_2$, $AgInS_2$, $CuInSe_2$, $AgInSe_2$)

have attracted much attention in recent years due to their unique optical properties, low toxicity, and potential applications in biological and optoelectronic fields [1 - 5]. Their photoluminescence (PL) spectra can be tunable from visible to near-infrared by changing the chemical composition, size, and reaction conditions (such as reaction temperature, reaction time, pH,…). Conventionally, the broad PL and the large Stokes shift of the ternary I-III-VI nanocrystals (NCs) are mainly related to the donor-acceptor-pair recombination or surface states [6]. Among the I-III-VI ternary NCs, there are numerous reports concerning metal sulfides, in particular on $CuInS_2$ and $AgInS_2$ NCs while the number of reports about ternary selenide NCs is more limited [4, 7 - 12]. This is related, on the one hand, to the smaller variety and commercial availability of suitable Se precursors and the higher oxidation sensitivity of selenide NCs. On the other hand, ternary sulfide NCs exhibited up till now superior optical properties to their selenide counterparts. Among the ternary selenide compounds, $AgInSe_2$ (AISe) has a direct band gap energy of 1.24 eV [13] giving access to a broad spectral range encompassing the visible and near-infrared covered by AISe NCs, which are therefore highly appealing for optoelectronic devices and bio-related applications. AISe NCs have been synthesized both in the organic phase and in water depending on their application fields. Most of the AISe syntheses have been reported in organic solvents implying the use of trioctylphosphine (TOP) and tributylphosphine (TBP) and require an inert atmosphere and high temperature. For example, Wood *et al*. [14] reported the fabrication of AISe QDs in TOP at 260 °C showing a broad emission of 600-1100 nm with full-width-half-maximum values (FWHM) from 180 to 260 nm and the PLQY ~21 %. After shelling with the ZnSe layer using a mixed solution of TOPSe and diethylzinc, the PLQY of AISe/ZnSe QDs enhanced to 53 % and 73 % for a thin and thick ZnSe shell, respectively. More recently, we synthesized AISe core and AISe/ZnS core/shell NCs in more common chemicals (dodecanethiol, oleylamine and 1-octadecene) at lower temperatures (<180 °C). By changing the reaction temperature from 100 °C to 180 °C, the AISe core NCs size could be adjusted from ~3.4 nm to 6.1 nm leading to tunable PL emission in a range of 647 - 807 nm, respectively. After overcoating with a thin ZnS layer, the PLQY of the obtained AISe/ZnS core/shell NCs increased up to 40 % along with high stability for extended storage for up to 12 months [15].

To overcome the intrinsic disadvantages of the preparation of AISe NCs in organic solvents (cost, environmental concerns), the aqueous synthesis of AISe NCs has received more attention in recent years. The aqueous synthesis approach is known as a cheaper, simpler, and much greener method in nature as it avoids the use of large quantities of organic solvents. However, aqueous synthesis of AISe QDs also has encountered challenges: due to difficulties in controlling the reaction rate, the obtained NCs have low PLQY and unstable optical properties. This is also the driving force that promoted recent research on the formation of high-quality water-soluble AISe NCs. For instance, Pan *et al.* reported the synthesis of water-soluble AISe/ZnS core/shell NCs using an electric pressure cooker [16]. The AISe/ZnS core/shell NCs exhibited PL emission in the range from 582 nm to 650 nm by changing composition with a maximum PLQY of 20 %. Zahn *et al*. synthesized AISe NCs capped by glutathione with PL emission tunable in the 650 - 750 nm region depending on the Ag:In ratios. Under optimized conditions, the PL QY reached 4 % for AISe core NCs and 12 % for AISe/ZnS core/shell NCs [17].

In this study, we propose a novel approach for the synthesis of AISe core and highly luminescent AISe/ZnS core/shell NCs in a 2-step procedure. First, the AISe core NCs were produced using both glutathione and citric acid as dual stabilizers at 96 °C for 20 min at different pH values of the reaction solution. The simultaneous presence of GSH and citric acid improved

significantly the PL properties of the AISe core NCs. After that, a ZnS layer was formed on the surface of the AISe NCs at 90 °C for 60 min to create an AISe/ZnS core/shell structure. During this step, the PLQY of the NCs increased by a factor of three and the obtained AISe/ZnS core/shell NCs exhibited long-term (more than 6 months) stability of their optical properties.

2. EXPERIMENTAL

2.1. Materials

Silver nitrate ($AgNO_3$, 99 %), indium chloride ($InCl_3$, 99.999 %), zinc acetate ($Zn(ac)_2$, 99 %), selenium powder (99.99 %), L-glutathione reduced (GSH, ≥ 98 %), ammonium hydroxide (NH_4OH, 28.0 - 30.0 %), citric acid (anhydrous, 99.5 %) were purchased from Sigma-Aldrich. Ethanol (99.5 %) and acetone (99 %) were purchased from Fisher. We used the chemicals as received without further purification.

2.2. Synthesis of AISe and AISe/ZnS core/shell NCs

AISe NCs were synthesized in an aqueous solution. Typical, 2.4 ml of 0.5 M GSH, 0.8 ml of 1 M $InCl_3$, and 5 ml of water were mixed in a three-necked flask. 5.0 M NH_4OH solution was added slowly to the mixture of In precursor until a white precipitate appeared, then the white precipitate gradually dissolved after vigorous mixing, forming a clear solution of the In complex. Next, 2 ml of 0.1M $AgNO_3$ was injected into the reaction mixture. All reactions were carried out in oxygen-free water degassed by nitrogen, and then 1.0 ml of fresh NaHSe solution (0.5 M) was added, which was prepared from selenium powder through a reduction reaction in $NaBH_4$ solution. Then, some drops of a 2.0 M aqueous solution of citric acid were added to adjust the pH in a range from 6 to 9. The reaction mixture was heated to 96 °C and kept at this temperature for 20 min under stirring to form AISe NCs. Next, the stock solution of Zn and S precursors were added gradually into the flask containing AISe core NCs at 90 °C under N_2 to grow the ZnS shell. This reaction solution was kept at 90 °C for 60 min and then cooled down to room temperature. The obtained AISe/ZnS NCs were collected by adding acetone into the NCs colloidal solution and then centrifuging. Finally, the precipitated NCs were re-dispersed in water for the characterization.

The stock solution for shelling the ZnS layer was prepared by mixing the mixture of 2.4 ml of 0.5M GSH, 0.8 ml of $Zn(ac)_2.2H_2O$ 1 M, and 0.8 ml of thiourea 1 M and adjusting pH to 7.

2.3. Characterization

Structural and morphology characterizations of AISe and AISe/ZnS NCs were analyzed by using X-ray diffraction (XRD, D8-ADVANCE, Bruker, Germany), X-ray photoelectron spectroscopy (XPS, VG ESCALAB 200i, Thermo Fisher Scientific), and transmission electron microscopy (TEM, Tecnai F20 Microscope). Photoluminescence (PL, Horiba iHR550) and UV-Vis-NIR absorption (Carry 350) spectroscopies were used to estimate the optical characteristics. A 355 nm laser was utilized as the excitation source for the PL measurement, and a thermoelectrically cooled Si-CCD camera (Synapse) was used to detect the PL signals. The PL QY values were calculated as indicated in our previous report [15].

3. RESULTS AND DISCUSSION

Our study aims to synthesize high-quality NCs emitting stable and strong luminescence in the red region (650 - 750 nm), which is an important spectral range for the production of lighting devices for plants, and bio-related applications [11, 18]. To tune the emission wavelength, we varied the Ag:In ratio from 1:1 to 1:10. The effect of Ag:In ratios on the emission wavelength and intensity has been reported earlier [8, 17, 19]. Hereafter, we focus on the characterization of the AISe NCs synthesized with the Ag:In molar ratio of 1:4, which showed the strongest PL in the targetted spectral range, and investigate the influence of pH on the PL properties.

In this work, the metal precursors for the preparation of the AISe NCs are $AgNO_3$ and $InCl_3$. The reactivities of the Ag^+ and In^{3+} cations with the Se precursor are different, leading to difficulties in controlling the formation of AISe NCs with the desired crystal structure and composition [1]. In this context, the presence of both GSH and citric acid played a crucial role in the reaction. Based on the hard and soft acids and bases (HSAB) principle [20], In^{3+} is a hard acid and citrate and OH^- are hard bases. In this case, the basicity of citrate is stronger than OH^-, resulting in the formation of indium-citrate complexes. Ag^+ is a soft acid and the thiol function in GSH is a soft base, so Ag^+ preferentially reacts with GSH to obtain Ag-GSH complexes. The formation of these In-citrate and Ag-GSH complexes enables balancing the reactivity of the metal cations with the Se anion [1], similar to the case of AIS NCs [21].

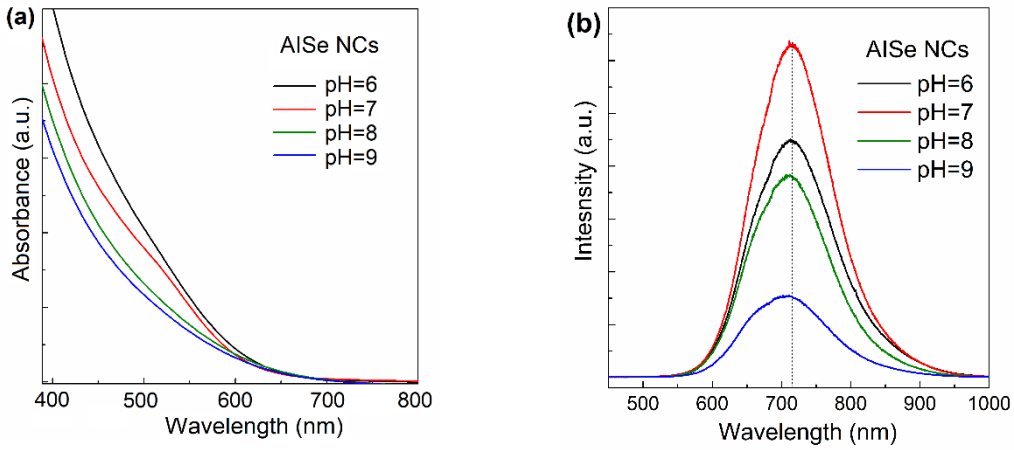

Figure 1. (a) Absorption and (b) PL spectra of AISe core NCs as a pH function.

Figure 1 shows the absorption and PL spectra of the synthesized AISe NCs at different pH values in the range of 6 to 9. As usual for ternary NCs, no well-defined excitonic absorption peaks are visible (Figure 1a). With increasing pH, the onset of the absorption bands remained unaffected while a decrease of absorption was observed in the 400 - 600 nm region. Only the pH 7 sample shows a distinct absorption shoulder in the 500 - 550 nm range. The PL peaks of AISe core NCs (Figure 1b) shift slightly from 715 nm to 705 nm with the increase of reaction pH from 6 to 9, respectively. The PL intensity of AISe core NCs at pH 7 is the strongest. When the pH value was lower than 7, GSH might be oxidized or hydrolyzed, leading to difficulty in forming the Ag-GSH complex. For pH values higher than 7, the OH^- concentration was increased in the reaction solution, which directly affected the stability and reactivity of the Ag-GSH and In-citrate complexes. Furthermore, surface bonding between the synthesized AISe NCs and the stabilizer as GSH, citrate was obstructed, resulting in producing a large number of surface

defects, thus enhancing non-radiative recombination effects and reducing the fluorescence intensity of AISe NCs [22]. At pH 7, the metal complexes performed well in balancing the reactivity of the metal cations while maintaining strong bonding between the AISe inorganic core and the GSH ligands, effectively passivating the surface defects of AISe NCs to improve their emission [23]. Therefore, the synthesized AISe NCs showed the best PL properties at pH 7.

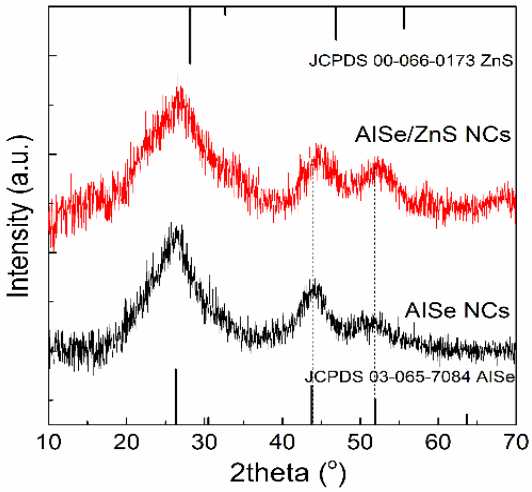

Figure 2. XRD patterns of AISe core and AISe/ZnS core/shell NCs synthesized at pH 7.

After finding the optimal pH value to synthesize AISe NCs, we proceeded to their overcoating with a ZnS shell to further enhance their PLQY. Figure 2 shows the XRD patterns of AISe and AISe/ZnS NCs synthesized at pH 7. The XRD pattern of AISe exhibits three main diffraction peaks at 2θ of 26.30°, 44° and 52° corresponding to the (111), (220) and (311) planes of the cubic $AgInSe_2$ structure (JCPDS 03–065–7084). After ZnS coating, these three diffraction peaks were slightly shifted to higher angles, which are closer to the typical XRD peaks of the cubic ZnS structure (JCPDS 00–066–0173). This shift has been widely observed in AISe/ZnS core/shell structures, indicating the successful growth of ZnS on the surface of AISe core NCs and the XRD results are in agreement with the published literature for AISe/ZnS core/shell NCs [24, 25].

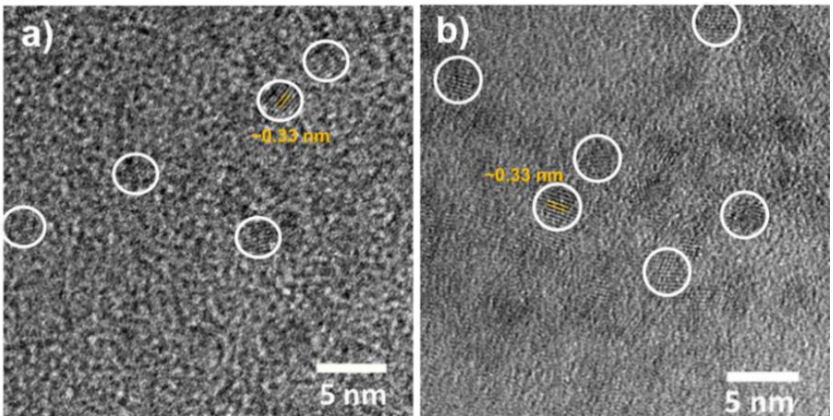

Figure 3. HRTEM images of (a) AISe core and (b) AISe/ZnS core/shell NCs synthesized at pH 7.

Figure 3 presents HRTEM images of the synthesized AISe and AISe/ZnS core/shell NCs at pH 7. It can be seen that the AISe core and AISe/ZnS core/shell NCs are spherical particles with an average diameter of 2.8 nm and 3.6 nm, respectively. The observed mean size increase of 0.8 nm corresponds to a ZnS shell thickness of around 1.3 monolayers. Both the synthesized core and core/shell NCs samples show good crystallinity and clear lattice fringes with the observed lattice spacing of ~0.33 nm, which matches the (111) plane of the cubic AISe NCs structure [26]. This fringe spacing is almost unchanged after shelling with the ZnS layer due to the ZnS lattice spacing of 0.31 nm being close to that of AISe.

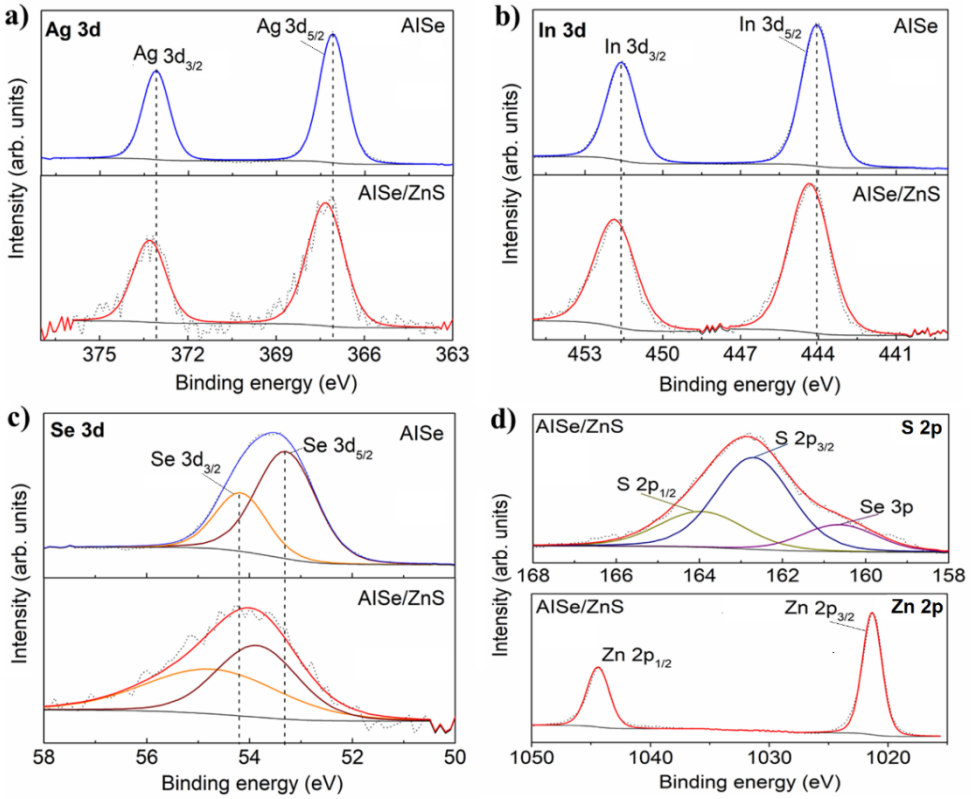

Figure 4. High-resolution XPS spectra of (a) Ag 3d, (b) In 3d, (c) Se 2p and (d) S 2p and Zn 2p core level of AISe core and AISe/ZnS core/shell NCs synthesized at pH 7.

The elemental states and chemical compositions of the synthesized NCs were investigated by XPS. Figure 4 presents the XPS spectra of the AISe NCs before and after ZnS shell growth. It can be seen clearly that the peaks of Ag, In and Se elements are shifted to higher binding energies after coating the AISe core with the ZnS shell (Figures 4(a - c)). Particularly, the double peaks of $3d_{5/2}$ and $3d_{3/2}$ at around 367.1 and 373.1 eV, 444.1 and 451.6 eV, 53.3 and 54.2 eV, respectively, which correspond to the existence of Ag^{+}, In^{3+} and Se^{2-} are in agreement with previous literature [15, 26 - 28]. After shelling with the ZnS layer, these peaks shift to higher energy by 0.2 eV for Ag and In, and by 0.5 eV for Se. This shift could be attributed to Zn^{2+} ions replacing Ag^{+} and In^{3+} ions or the formation of the ZnS shell leading to a change in the electronic environment in the AISe NCs. Given the observed blue-shift of the PL peak upon shell growth (vide infra), the former hypothesis is most likely, consistent with reports on AIS/ZnS NCs [19]. These results are consistent with the shift in the XPS spectra of Cu, In, Se

and S elements reported for CISeS/ZnS and ZnCISeS/ZnS NCs [28]. Besides, the Zn and S signals were detected and shown in Figure 4d. The binding energy peaks of Zn $2p_{3/2}$ and Zn $2p_{1/2}$ at 1021.3 eV and 1044.4 eV are attributed to the presence of Zn^{2+} species in the sample [15]. The peaks located at around 162.8 eV and 164.0 eV originate from S $2p_{3/2}$ and S $2p_{1/2}$ of S^{2-} species in the Zn-S bond [15, 29]. These XPS results confirm the existence of the ZnS layer on the surface of the AISe NCs to form the AISe/ZnS core/shell structure.

The absorption and PL spectra of the AISe core and AISe/ZnS core/shell NCs prepared at pH 7 are shown in Figure 5. The absorption of AISe/ZnS NCs (Figure 5a) is very similar to the AISe core NCs. However, the PL spectrum of the AISe/ZnS core/shell NCs (Figure 5b) exhibits a distinct blue shift from 715 to 680 nm compared to the core, with an emission line width of ~130 nm.

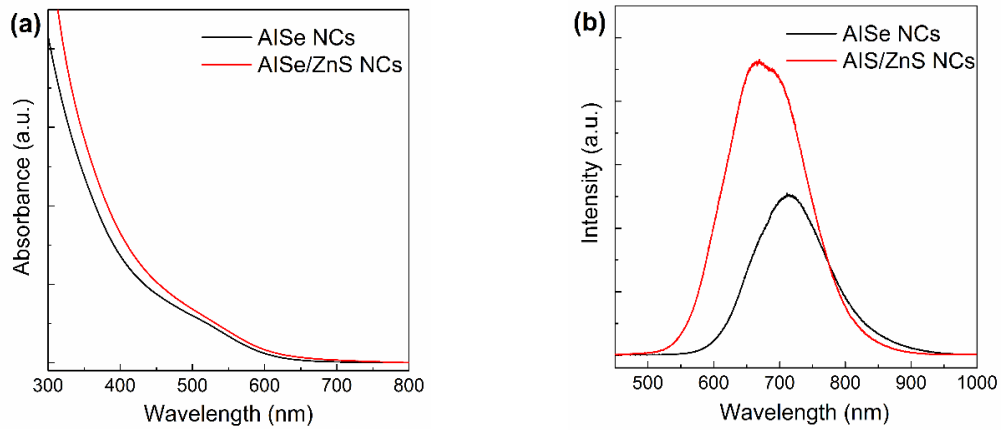

Figure 5. (a) Absorption and (b) PL spectra of AISe core and AISe/ZnS NCs synthesized at pH 7.

The blue shift indicates the formation of Ag-In-Zn-Se alloyed NCs during the growth of the ZnS shell by cation exchange between Ag^{+} or In^{3+} and Zn^{2+} ions. Most importantly, the PLQY increased remarkably up to 30 % after coating the ZnS shell on the AISe surface, which was a more than threefold enhancement compared to the AISe core NCs. This increase can be attributed to the ZnS shell passivating dangling bonds and other defects on the surface of the AISe core NCs [7, 15, 16], which may be further enhanced by the formation of the alloyed core. Moreover, the stability of the optical properties of NCs was significantly improved after the growth of the ZnS shell as shown in Table 1.

Table 1. PL QY of AISe core and AISe/ZnS core/shell NCs with storage time under ambient air.

Samples	AISe NCs	AISe/ZnS NCs
QY (%) as-prepared	10	30
QY (%) after 1 month	1	27
QY (%) after 3 months	0	25
QY (%) after 6 months	0	22

Concretely, the PLQY of the bare AISe NCs was quenched rapidly after 1 month, with almost no fluorescence remaining, while the QY of the AISe/ZnS core/shell NCs was only

reduced by around 26 % compared to the initial value after 6 months' storage under ambient air conditions. Thus, the ZnS shell plays an important role in passivating effectively the surface to enhance both the PLQY and the stability of the emission properties.

These results were compared to those reported in the literature as shown in Table 2. Overall, with the hot-injection method in organic solvents, the PLQY of the obtained NCs is higher than that of the water-soluble NCs [14, 15, 30]. However, the organic syntheses require higher temperatures and more expensive chemicals and solvents, which in addition present risks for human health and the environment. In comparison with the reported AISe and AISe/ZnS(Se) NCs syntheses in water, our method is simpler and yields a higher PLQY. While most methods apply hydrothermal conditions using temperatures > 100 °C and elevated pressure [8, 16, 31], here temperatures below 100 °C were applied at ambient pressure. The key aspect of the present procedure for synthesizing AISe and AISe/ZnS NCs of high quality is the use of GSH and citric acid as dual stabilizers during the precursor preparation.

Table 2. Comparison of the optical properties of the AISe core and AISe/ZnS core/shell NCs synthesized in this work with other reports.

Sample	**Synthesis conditions**	**λ_{PL} (nm)**	**FWHM (nm)**	**Max. QY (%) at PL peak (nm)**	**Ref.**
$AgInSe_2$ NCs $AgInSe_2$/ZnS NCs	Aqueous solution at 96 °C for core and 90 °C for core/shell	Core: 715 Core/shell: 680	130	Core: 10 % Core/shell: 30 %	This work
Ag–In–Se QDs Ag-In-Se/ZnS QDs	Aqueous solution at 98 °C	Core: 700 Core/shell: 650	120	Core: 4 % Core/shell: 12 %	[17]
$AgInSe_2$ QDs $AgInSe_2$/ZnS QDs	Hydrothermal at 120 °C (180 kPa) for core and 80 °C for core/shell	Core/shell: orange- and red-emitting PL	100	Core/shell: 10.1 - 20.5 %	[16]
$AgInSe_2$ QDs $AgInSe_2$/ZnSe QDs	Hydrothermal at 240 °C for core and 200 °C for core/shell	Core: 701 Core/shell: 675	150	Core: 0.62 % Core/shell: 5.6 %	[8]
$AgInSe_2$ QDs $AgInSe_2$/ZnS QDs	Hydrothermal at 120 °C for core and 80 °C for core/shell	Core/shell: 705	170	Core/shell: 10.16 %	[27]
$AgInSe_2$ NCs $AgInSe_2$/ZnS NCs	Hot injection at 100 - 180 °C for core and 150 °C for core/shell	Core: 647 - 807 Core/shell: 610 - 762	Core: 159 - 200 Core/shell: 119 - 180	Core: 9 % (713) Core/shell: 40 % (671)	[15]
$Ag_3In_5Se_9$ NCs $Ag_3In_5Se_9$/ZnSe NCs	Hot injection at 260 °C	640 - 1150	> 260	Core: 21 % (950) Core/shell: 73 % (640)	[14]
$AgInSe_2$/ZnS QDs	Hot injection at 175 - 250 °C	700 - 820	200	Core: 10 % (800) Core/shell: 40 % (775)	[30]

4. CONCLUSION

In conclusion, water-soluble AISe NCs have been synthesized by a simple and economical route at 96 ℃ within 20 min. Using GSH and citric acid as dual stabilizers to balance the reactivity of the precursor metal cations in aqueous medium produced AISe core NCS with a size of 2.8 nm. Optimization of the pH value of the reaction solution yielded the strongest emissive AISe core NCs showing a PLQY of 10 % at pH 7. AISe/ZnS core/shell NCs with size 3.6 nm were produced at 90 ℃ within 60 min by injecting slowly the ZnS precursor stock solution into the colloidal solution of the AISe core NCs. They exhibit excellent luminescence properties, peaking at 680 nm with PLQY as high as 30 % and retaining ~83 % after 3 months and ~73 % after 6 months of storage under ambient conditions in air. The ZnS shell plays a dual role in passivating effectively surface defects to enhance the PLQY and to protect the AISe core NCs against degradation/oxidation. The optical properties of obtained AISe/ZnS core/shell NCs are promising for the production of lighting devices for plants, and for bio-related applications such as in vivo imaging.

Acknowledgements. This work has been supported by Vietnam Academy of Science and Technology under grant No. TĐHYD0.04/22-24. The authors acknowledge Objective Lab for Agriculture-Bio-Medicine and Energy of VAST/IMS for using the Lab's equipment. P.R. acknowledges financial support from Labex ARCANE (ANR-11-LABX-0003).

CRediT authorship contribution statement. Tran Thi Thu Huong: synthesis samples, Investigation. Nguyen Thi Hiep: Formal analysis, review & editing. Nguyen Thu Loan, Le Van Long, Jae Yup Kim: Investigation, Formal analysis. Nguyen Thanh Tung: Formal analysis, Funding acquisition. Ung Thi Dieu Thuy: Formal analysis, conceptualization, Writing manuscript. Peter Reiss, Nguyen Quang Liem: Supervision, review & editing.

Declaration of competing interest. The authors declare that they have no known competing financial interests or personal relationships that could have appeared to influence the work reported in this paper.

REFERENCES

1. May B. M., Bambo M. F., Hosseini S. S., Sidwaba U., Nxumalo E. N., and Mishra A. K. - A review on I–III–VI ternary quantum dots for fluorescence detection of heavy metals ions in water: optical properties, synthesis and application, RSC Adv. **12** (2022) 11216-32.
2. Jain S., Bharti S., Bhullar G. K., and Tripathi S. K. - I-III-VI core/shell QDs: Synthesis, characterizations and applications, J. Lumin. **219** (2020) 116912.
3. Moodelly D., Kowalik P., Bujak P., Pron A., and Reiss P. - Synthesis, photophysical properties and surface chemistry of chalcopyrite-type semiconductor nanocrystals, J. Mater. Chem. C **7** (2019) 11665-11709.
4. Li L., Daou T. J., Texier I., Tran T. K. C., Nguyen Q. L., and Reiss P. - Highly Luminescent CuInS2/ZnS Core/Shell Nanocrystals: Cadmium-Free Quantum Dots for In Vivo Imaging, Chem. Mater. **21** (2009) 2422-2429.
5. Islas-Rodriguez N., Muñoz R., Rodriguez J. A., Vazquez-Garcia R. A., and Reyes M. - Integration of ternary I-III-VI quantum dots in light-emitting diodes, Front. Chem. **11** (2023) 1106778.
6. Hong S. P., Park H. K., Oh J. H., Yang H., and Do Y. R. - Comparisons of the structural and optical properties of o-AgInS2, t-AgInS2, and c-AgIn5S8 nanocrystals and their

solid-solution nanocrystals with ZnS, J. Mater. Chem. **22** (2012) 18939-49.

7. Song W. S. and Yang H. - Efficient white-light-emitting diodes fabricated from highly fluorescent copper indium sulfide core/shell quantum dots, Chem. Mater. **24** (2012) 1961-7.
8. Oluwafemi O. S., May B. M. M., Parani S., and Tsolekile N. - Facile, large scale synthesis of water soluble AgInSe2/ZnSe quantum dots and its cell viability assessment on different cell lines, Mater. Sci. Eng. C **106** (2020) 110181.
9. Uematsu T., Wajima K., Sharma D. K., Hirata S., Yamamoto T., Kameyama T., Vacha M., Torimoto T., and Kuwabata S. - Narrow band-edge photoluminescence from AgInS2 semiconductor nanoparticles by the formation of amorphous III–VI semiconductor shells, NPG Asia Mater. **10** (2018) 713-26.
10. Huong T. T. T., Loan N. T., Ung T. D. T., Tung N. T., Han H., and Liem N. Q. - Systematic synthesis of different-sized AgInS2/GaSx nanocrystals for emitting the strong and narrow excitonic luminescence, Nanotechnology **33** (2022) 355704.
11. Huong T. T. T., Loan N. T., Van Long L., Phong T. D., Ung Thi Dieu T., and Liem N. Q. - Highly luminescent air-stable AgInS2/ZnS core/shell nanocrystals for grow lights, Opt. Mater. (Amst). **130** (2022) 112564.
12. Loan N. T., Huong T. T. T., Luong M. A., Han H., Ung T. D. T., and Liem N. Q. - Double-shelling AgInS2 nanocrystals with GaSx/ZnS to make them emit bright and stable excitonic luminescence, Nanotechnology **34** (2023) 315601.
13. Sanmartín-Matalobos J., Bermejo-Barrera P., Aboal-Somoza M., Fondo M., García-Deibe A. M., Corredoira-Vázquez J., and Alves-Iglesias Y. - Semiconductor Quantum Dots as Target Analytes: Properties, Surface Chemistry and Detection, Nanomaterials **12** (2022) 2501.
14. Yarema O., Yarema M., Bozyigit D., Lin W. M. M., and Wood V. - Independent composition and size control for highly luminescent indium-rich silver indium selenide nanocrystals, ACS Nano **9** (2015) 11134-42.
15. Huong T. T. T., Hiep N. T., Loan N. T., Han H., Thao N. T., Thuy U. T. D., and Liem N. Q. - Improved stability and luminescent efficiency of AgInSe2 nanocrystals by shelling with ZnS, Adv. Nat. Sci. Nanosci. Nanotechnol. **14** (2023) 25017.
16. Kang X., Yang Y., Huang L., Tao Y., Wang L., and Pan D. - Large-scale synthesis of water-soluble CuInSe 2/ZnS and AgInSe 2/ZnS core/shell quantum dots, Green Chem. **17** (2015) 4482-8.
17. Raievska O., Stroyuk O., Dzhagan V., Solonenko D., and Zahn D. R. T. - Ultra-small aqueous glutathione-capped Ag–In–Se quantum dots: luminescence and vibrational properties, RSC Adv. **10** (2020) 42178-93.
18. Mattera L., Bhuckory S., Wegner K. D., Qiu X., Agnese F., Lincheneau C, Senden T, Djurado D, Charbonniere L J, Hildebrandt N, Reiss P. - Compact quantum dot-antibody conjugates for FRET immunoassays with subnanomolar detection limits, Nanoscale **8** (2016) 11275-11283.
19. Rivaux C, Akdas T, Yadav R, El-Dahshan O, Moodelly D, Ling W L, Aldakov D and Reiss P. - Continuous Flow Aqueous Synthesis of Highly Luminescent AgInS2 and AgInS2/ZnS Quantum Dots, J. Phys. Chem. C **126** (2022) 20524-20534.
20. Yarema O., Yarema M., and Wood V. - Tuning the composition of multicomponent semiconductor nanocrystals: The case of I–III–VI materials, Chem. Mater. **30** (2018) 1446-61.

21. Dhamo L., Wegner K. D., Würth C., Häusler I., Hodoroaba V. D., Ute R. G. - Assessing the influence of microwave-assisted synthesis parameters and stabilizing ligands on the optical properties of AIS/ZnS quantum dots, Scientifc Reports **12** (2022) 22000.
22. Xue T., Shi Y., Guo J., Guo M., and Yan Y. - Preparation of AgInS2 quantum dots and their application for Pb2+ detection based on fluorescence quenching effect, Vacuum **193** (2021) 110514.
23. Xiong W. W., Yang G. H., Wu X. C., and Zhu J. J. - Microwave-assisted synthesis of highly luminescent AgInS 2/ZnS nanocrystals for dynamic intracellular Cu (ii) detection, J. Mater. Chem. B **1** (2013) 4160-5.
24. Kang X., Yang Y., Huang L., Tao Y., Wang L., and Pan D. - Large-scale synthesis of water-soluble CuInSe2/ZnS and AgInSe2/ZnS core/shell quantum dots, Green Chem. **17** (2015) 4482-8.
25. Che D., Zhu X., Wang H., Duan Y., Zhang Q., and Li Y. - Aqueous synthesis of high bright and tunable near-infrared $AgInSe_2$–ZnSe quantum dots for bioimaging, J. Colloid Interface Sci. **463** (2016) 1-7.
26. Pei-Ni L., Anil V. G., Jia-Yaw C. - Direct aqueous synthesis of quantum dots for high-performance $AgInSe_2$ quantum-dot-sensitized solar cell, Journal of Power Sources **354** (2017) 100-107.
27. Yang Y., Liu Y., Mao B., Luo B., Zhang K., Wei W., Kang Z., Shi W., Yuan S. - Facile Surface Engineering of Ag–In–Zn–S Quantum Dot Photocatalysts by Mixed-Ligand Passivation with Improved Charge Carrier Lifetime, Catal. Lett. **149** (2019) 1800-1812.
28. Wang K., Liang Z., Li J., Xu X., Cheng X., Jin H., Xu D., and Xu G. - Formation and photoluminescence properties of colloidal ZnCuIn(SexS1 2 x)2/ZnS nanocrystals with gradient composition, J. Mater. Sci. **54** (2019) 2037-2048.
29. Priyanka U. L., Sachin D., Sunit R., Nandu C., Bharat K. - A Novel combined thermal evaporation and solvothermal approach to produce highly crystalline and compact CIG(S1-xSex)2 thin films, Applied Materials Today **35** (2023) 101932.
30. Deng D., Qu L., and Gu Y. - Near-infrared broadly emissive AgInSe2/ZnS quantum dots for biomedical optical imaging, J. Mater. Chem. C **2** (2014) 7077-85.
31. Ncapayi V., Ninan N., Lebepe T. C., Parani S., Girija A. R., Bright R., Vasilev K., Maluleke R., Tsolekile N., Kodama T., and Oluwafemi O. S. - Diagnosis of Prostate Cancer and Prostatitis Using near Infra-Red Fluorescent AgInSe/ZnS Quantum Dots, Int. J. Mol. Sci. **22** (2021) 12514.